

文章编号 1004-924X(2007)04-0615-07

激光主动成像图像的多帧后处理算法研究

王 智¹, 贾书洪², 张晓辉³, 金 光¹, 张立平¹, 夏 辉⁴

(1. 中国科学院 长春光学精密机械与物理研究所, 吉林 长春 130033; 2. 空军航空大学 基础部, 吉林 长春 130033; 3. 吉林省探矿机械厂 经营计划科, 吉林 长春 130012; 4. 青岛大学 信息工程学院, 山东 青岛 266071)

摘要: 在确定激光器的发散角度、脉冲峰值功率、接收光学系统的参数以及确定激光器和接收光学系统的几何配置后, 激光主动成像系统要想得到更远距离更高分辨率的微弱目标的图像, 就只受微弱目标的探测成像及处理技术的制约, 因为在较长的距离和有限的激光能量下, 不可能立刻照明整个目标场景, 接收成像端 CCD 上每个像素接收到的光照度也不可能达到相当的水平。为了在特定的脉冲激光能量下增加成像系统的成像距离, 同时减轻大气扰动对成像分辨率的影响, 研究了一种独特的图像处理算法, 用激光多脉冲来获取整个目标场景的图像, 采用辐射量来确定每次曝光时间内最大景物照明区域, 这种独特的多帧后处理算法, 可以在大气扰动和连续散粒噪声影响下, 得到比传统连续照明方式更高分辨率的图像。

关键词: 激光主动成像; 多帧后处理; 图像配准

中图分类号: TP391.4 **文献标识码:** A

Multiframe postprocessing algorithm of laser active imaging images

WANG Zhi¹, JIA Shu-hong², ZHANG Xiao-hui³, JIN Guang¹, ZHANG Li-ping¹, XIA Hui⁴

(1. *Changchun Institute of Optics, Fine Mechanics and Physics, Chinese Academy of Sciences, Changchun 130033, China*; 2. *Fundamental Department, Aviation University of Air Force, Changchun 130022, China*; 3. *Management and Plan Department, Jilin Province Geological Prospecting Machinery Works, Changchun 130012, China*; 4. *College of Information Engineering, Qingdao University, Qingdao 266071, China*)

Abstract: After fixing on the divergent angle, peak power of laser pulse, parameters of received optical system and the geometrical configuration between laser and received optical system, a faint target image of longer range with higher resolution obtained by active imaging system is constrained by imaging and processing technologies. With longer range and limited laser energy, it is impossible to illuminate the entire scene at once, and the illuminance obtained by each receiver pixel of CCD can not achieve an adequate level. In order to increase the imaging range of imaging system with given per-pulse laser energy, and to reduce atmospheric turbulence effects on image resolution, multi pulses may be employed to obtain image data over the whole scene and radiometric conceptions are used to establish the maximum scene illumination region during each exposure. A unique multiframe postprocessing technique is

收稿日期: 2006-11-22; 修订日期: 2007-03-18.

Foundation item: Supported by National Natural Science Foundation of China (No. 60575025)

investigated in this paper. It is shown that in the presence of atmospheric turbulence and coherent speckle effects, this approach can produce superior results to conventional scene flood illumination.

Key words: laser active imaging; multiframe postprocessing; image registration

1 Introduction

Laser active imaging technology can be used to augment presently available sensor suites in surveillance system, which has advantages over traditional passive imaging system based on images in some work environments. For instance; imaging under the condition of bad visibility and pitchblack night; imaging in scattering medium; detecting the faint target in long range and the small target in deep space, etc. No matter what passive imaging system or active imaging system, the energy of reflective signal by target is a key issue. Under former environments, the reason that passive imaging system can't work is weak energy reflected by target, does not meet the need of even if the most sensitive imaging sensor. To overcome the disadvantage of passive imaging system, an additional illuminator source is added to illuminate small and dark target in long range, and augment useful signal reflected by target.

Laser active illuminated imaging is not a new concept, from the naissance of the first laser, laser active imaging was researched overseas, it has been researched for several decades. The technology is very mature in U. S. , Canada and other countries, and is used in martial reconnaissance, search and succor etc. , even is equipped in army. The latest information presents that laser active imaging is used in reconnaissance, illumination at $1.4\sim 2.0\ \mu\text{m}$ is easily accomplished using a narrow-pulsed Nd: YAG laser, and the instrument can be optimized for imaging at ranges out to 50 km.

From the view of pertinent reports at home, research on laser active imaging is beginning, most are concept research, with many lab mark.

After fixing on laser energy, divergent angle, parameters of received optical system and geometrical configuration between laser and received optical system, atmospheric turbulence is the key factor to affect image resolution and signal to noise. Atmospheric turbulence over long slant paths can introduce severe distortions and anisoplanatic effects into the imagery. Coherent interference from the reflected laser illumination gives the resulting images a speckled intensity distribution, which acts as an added noise. With augment of imaging distance, energy that reflected by object imaging area is decreased, then laser energy needs to be increased. However at the same time that augment illuminator energy, background scatter induced by backscatter is increased, even covered reflected signal of object. Over the past few years many researchers have been working on approaches to overcome these limitations and extend the useful range of a laser active illuminated imaging system, quicken applied step of the laser active illuminated imaging system.

2 Experiment system and collection object's images

The faint target at long range is imaging under conditions of night, for long range with limited illuminator energy, it may not be possible to illuminate the entire scene at once and still achieve an adequate level of return at each receiver pixel. Multiple pulses may be required to obtain image data over the whole scene, spending a corresponding longer acquisition time. In addition multiple scene illuminations along with postprocessing can be used to alleviate coherent speckle and atmosphere-induced anisoplanatic

effects.

Therefore, based on overseas researching direction, a multiframe acquisition and processing approach is developed. Fig. 5 is a block diagram of the postprocessing algorithm. By scanning of laser illuminator, multi-illuminated regions which can cover entire object scene are produced. Simple illuminated model and radiometric considerations are used to establish the maximum scene illumination region during each exposure, to ensure that reflected signal of object can not be covered by backscatter.

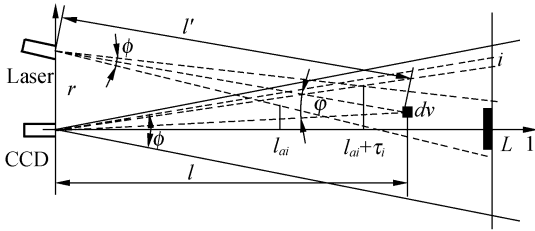


Fig. 1 Laser active illuminated imaging model

In this experiment, the laser active imaging system consists of parts below: laser illuminator (wavelength: 532 nm), receiver optical system, CCD camera, data collecting, processing and displaying part. The equipment distributing is shown as Fig. 1. After fixing on the divergent angle of laser, peak value power of laser, parameters of received optical system and geometrical configuration (see r in Fig. 1) between laser and received optical system, faint target image of longer range with higher resolution obtained by active imaging system is constrained by the technology of imaging and processing of faint target. To obtain higher resolution image of faint target at longer range, a unique image processing method is needed to acquire and postprocess multipulses imaging data of target.

In the process of acquiring image data, simple illuminated model and radiometric considerations are used to establish the maximum scene illumination region during each exposure (sub region - sub image). The simple laser illuminated

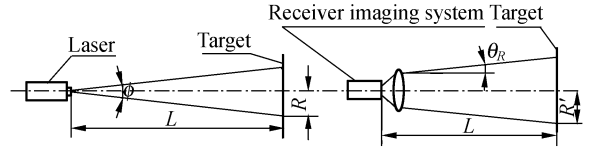


Fig. 2 Simple laser active imaging model

imaging model is shown in Fig. 2.

The laser divergent angle is ϕ , the distance between target and laser is L , radius of laser facula at where target located is R ,

$$R = L \cdot \tan(\phi/2), \quad (1)$$

Then laser facula diameter where target located is:

$$D = 2R = 2L \times \tan(\phi/2) \approx L \times \phi, \quad (2)$$

Based on geometrical optics theory, the area of facula where target located is:

$$S_o = \pi R^2 = \frac{\pi L^2 \phi^2}{4}, \quad (3)$$

Assumed transmitting that laser in air abide geometrical optics law; the atmosphere is even and isotropy; the distribution of laser energy is almost even, then irradiation of laser facula where L :

$$E_s = \frac{0.838 \cdot P_o}{S_o} \cdot \tau_i \cdot \tau, \quad (4)$$

Where, 0.838 is power percent distributed in the first Airy facula; P_o is power of laser; τ_i is permeation radio of emissive optic system; τ is one way permeation radio of atmosphere.

Assumed that A_r is valid received area of received telescope, θ_R is field of vision of received optic system, if laser located at where received telescope locates, then facula area where target locates is :

$$S_R = \pi(L \cdot \tan(\theta_R/2))^2 \approx \frac{\pi L^2 \theta_R^2}{4}, \quad (5)$$

Then the received reflected light irritation on imaging sensor is:

$$E_{AR} = \frac{E_s \cdot S_o \cdot \tau_o \cdot A_r \cdot \tau \cdot \tau_r}{S_R}, \quad (6)$$

Where, τ_o is reflected radio of object; τ_r is permeation radio of received optic system; A_r is valid received area of received telescope.

Based on conversion formula between irrita-

tion and illumination $\omega/m^2 = 21.5 \text{ lx}$, the reflected illumination can be presented as E_{OR} .

$$E_{OR} = E_{AR} \times 21.5(\text{lx}), \quad (7)$$

The reflected light irritation is converted to light illumination, compared with the minimum light illumination of CCD camera, the relationship between distance L and maximum illuminat-

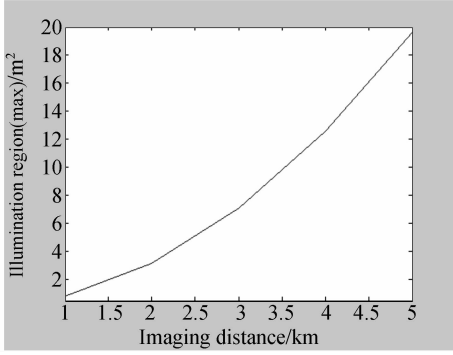


Fig. 3 Relationship between imaging distance L and maximum illuminated region

ed region is obtained.

In night, laser active imaging experiment is processed aim to target at 3 km range, under the condition as presented in table 1, the relation figure between the light illumination received by CCD and the imaging range is as Fig. 4.

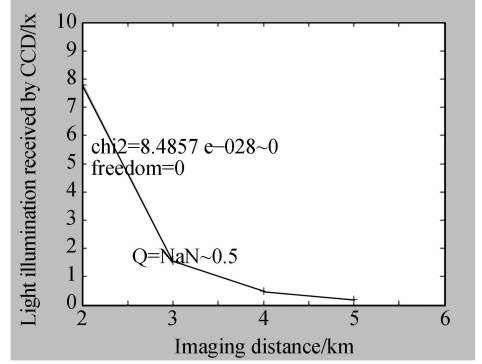


Fig. 4 Relationship between light illumination received by CCD and imaging range

Tab. 1 Parameters and atmospheric conditions of laser active imaging

L (km)	φ (mrad)	ψ (mrad)	r (m)	Wind (m/s)	Humidity (%)	Visibility (km)	β_{sc} (km^{-1})	β_{ex} (km^{-1})
3.0	1.0	10	0.5	1.0	70	0.05	0.0315	0.164

3 Multiframe postprocessing algorithm

In the process of acquisition of multiframe image data of object, the receiver focal plane array is fixed, only the illuminator moves during the scan process. Assumed that we have m incoherent subimages that together cover the entire scene. Each of the subimages can be described by the model:

$$i_k = (o * \text{beam}_k) * h_k |_{k=1, \dots, m}, \quad (8)$$

Where i_k is the k th subimage, o is the complete image of the scene, h_k is the k th long-exposure atmospheric point spread function associated with the subimage, and beam_k is the illuminator far-field intensity profile shifted to the k th illumination region. Given the ensemble i_k ob-

tained from the speckled images as described above, our goal is to obtain an estimate of o , which we denote \hat{o} , and an estimate of the point spread function ensemble, which we denote \hat{h}_k . We can obtain beam_k from shifted versions of the measured far-field illuminator intensity profile. In addition, we have the constraints that the estimate \hat{o} and \hat{h}_k must be real and positive.

Fig. 5 is a block diagram of the multiframe postprocessing algorithm. The inner loop of the block diagram is the standard blind deconvolution algorithm, but with the additional step, namely the relationship between the entire scene and sub images. Known from the convolution theory, All deconvolution operations are performed in the Fourier domain, since convolution transforms to multiplication. Uppercase letters represent Fourier-domain quantities, while lowercase letters pertain to the space domain. The

real-positive constraints are imposed in the space domain. A standard fast Fourier transform (FFT) algorithm is used to move back and forth between the two domains.

The preprocessing to the multiframe images begins the whole algorithm, the collected images are preprocessed to correct for pixel-to-pixel variation in the response. The preprocessing consists of a two-point calibration and a bad-pixel replacement scheme, which consisted in replacing the bad pixels with a weighted average of their eight neighbor pixels. In order to mitigate aliasing, we use a resolution-enhancement preprocessing step^[2]. The corrected data are $2 \times$ by $2 \times$ the size of the original array. This array is then inverse-Fourier-transformed. It can be shown that when one performs ensemble averages in the presence of frame-to-frame translation jitter, the resulting averages have a resolution greater than the original pixel sampling.

The first block within the outer loop represents in each incoherent subregion, image registration and average are operated to form incoherent subimage estimate. Next we initialize the iterative blind deconvolution algorithm^[3]. The initial estimate of the object \hat{o} is the sum of all the subimages obtained from the first block. Next we add the step to take account of the scanning illuminator and then form the initial estimates of the point spread functions using a regularized least-squares deconvolution, where ε_2 is a regularization constant to prevent the numerator from going to zero. The point spread functions are then transformed to the space domain, and real-positive constraints imposed.

The next block is inner loop of postprocessing algorithm, a standard blind deconvolution iterative algorithm. If one is unfamiliar with blind deconvolution methods, it is not intuitively obvious that the above algorithm should converge. However, weak convergence of blind deconvolution algorithms has been demonstrated^[4], and numerous experiments have confirmed its utili-

ty. It is the constraints that the estimates \hat{o} and \hat{h}_k must be real and positive, applied at each iteration step, that allow the algorithm to proceed.

We have found that improved performance can be obtained by iterating the outer loop of Fig. 5 several times. Once the inner loop has converged, the \hat{i}_k estimates are used as the starting point of the correlate-shift-and-add step to obtain new i_k , to provided a new estimate \hat{o} .

After obtaining all incoherent images estimated for each of the regions. The different subimages witch after preprocessing operation must then be stitched together.

The advantages of this algorithm are: multiframe averaging of each subregion based on image registration can mitigates coherent speckle effects. Anisoplanatic effects of the atmospheric turbulence are mitigated by an algorithm that stitches together each of the resulting subimages, allowing for independent atmospheric distortions over each subregion.

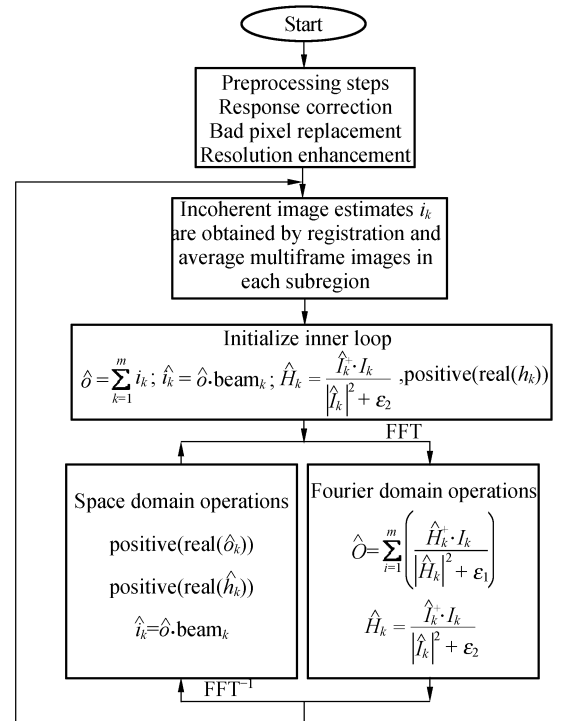
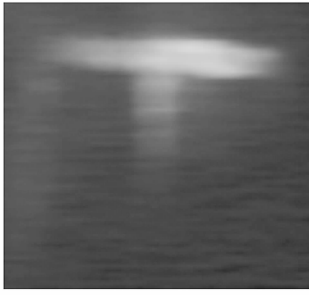
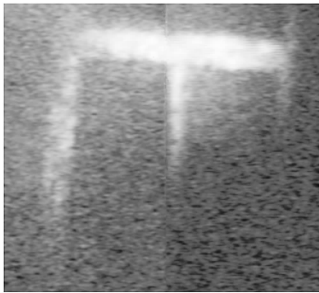


Fig. 5 Block diagram of multiframe processing algorithm using Ayers-Dainty blind deconvolution



(a) Entire target scene before multiframe postprocessing
(SNR 22.1961 dB)



(b) Entire scene after postprocessing
(SNR 33.850228 dB)

Fig. 6 Comparison of (a) before postprocessing and
(b) after postprocessing

In this section the results of multiframe image reconstructions are given. The active image data were collected at about 11 P. M. so that no solar background contaminated the images.

Fig. 6 shows the postprocessed results from 3-km target multiframe images.

4 Conclusion

The imagery presented here demonstrates nighttime laser-illuminated imagery at ranges out to 3 km. A $0.532 \mu\text{m}$ laser illuminator was used to provide the active illuminator source. The quality of the laser-illuminated imagery is limited primarily by the following: (1) laser backscatter from aerosols, (2) speckle noise due to the coherent illumination, (3) atmospheric distortions, (4) radiometric return. In this paper, we have demonstrated a multiframe iterative post-processing algorithm that addresses all the above issues except the laser backscatter. The laser backscatter problem could best be handled by gating the receiver detector.

In this experiment, a particular illuminator energy, a receiver optic system and the geometrical configuration between illuminator and receiver scan the system to obtain illuminators of the entire desired scene. Each region of the scene is reilluminated to perform multiframe postprocessing to mitigate speckle and atmospheric turbulence effects.

References:

- [1] DAVID D, STEVE B. Long-range laser illuminated imaging: analysis and experimental demonstrations[J]. *Opt. Eng.*, 2001,40(6):1001-1009.
- [2] STERN A, KEMPNER E, SHUKRUN A, *et al.*. Restoration and resolution enhancement of a single image from a vibration-distorted image sequence[J]. *Opt. Eng.*, 2000,39(9):2451-2457.
- [3] AYEYS G, DAINTY J, Iterative blind deconvolution method and its applications[J]. *Opt. Lett.*, 1998,13(7):547-549.
- [4] SCHULTZ T, Multiframe blind deconvolution of astronomical images[J]. *J. Opt. Soc. Am. A*, 1993,10(5):1064-1073.
- [5] WANG Z, JIN G, SUN X W. An algorithm of image segmentation for overlapping grain image[J]. *Opt. Precision Eng.*, 2005,13(5):592-598.
- [6] WANG Z, YANG J, JIN G. Technology of laser active illuminated imaging[J]. *J. Changchun Univ. Sci. Technol.*, 2004,27(2):31-34.
- [7] WANG Z, JIN G, YANG J. Laser active illuminated imaging: technological analysis and experimental demonstra-

tions[J]. *J. Changchun Univ. Sci. Technol.*, 2004, 27(4): 101-104.

- [8] SUN H Y, ZHOU D B, LI S L. Method for sequence image coalescence[J]. *Opt. Precision Eng.*, 2000, 8(1): 35-37.

Brief professional biography of the author: WANG Zhi(1978-), male, was born in Shandong province, received his PhD degree in Changchun Institute of Optics, Fine Mechanics and Physics, Chinese Academy of Sciences. His main interests are active imaging and precision mechanics designing. E-mail: wz7835@sohu.com

(本栏目编辑 黄廉卿)